Turbocharging synaptic transmission

James Rothman, Kirill Grushin, Manindra Bera, Frederic Pincet

"Turbocharging Synaptic Transmission"

By

James E. Rothman[1], Kirill Grushin[1], Manindra Bera[1] and Frederic Pincet[1,2]

[1]Nanobiology Institute and Department of Cell Biology, Yale University
[2] Laboratoire de Physique de l'Ecole normale supérieure, ENS, Université PSL, CNRS, Sorbonne Université, Université Paris Cité, F-75005 Paris, France

Abstract

Evidence from biochemistry, genetics, and electron microscopy strongly supports the idea that a ring of Synaptotagmin contributes importantly to clamping and release of synaptic vesicles for synchronous neurotransmission. Recent direct measurements in cell-free systems suggest there are 12 SNAREpins in each ready-release vesicle, consisting of 6 peripheral and 6 central SNAREpins. The 6 central SNAREpins are directly bound to the Synaptotagmin ring, are directly released by Ca^{++}, and they initially open the fusion pore. The 6 peripheral SNAREpins are indirectly bound to the ring, each linked to a central SNAREpin by a bridging molecule of Complexin. We suggest that the primary role of peripheral SNAREpins is to provide additional force to "turbocharge" neurotransmitter release, explaining how it can occur much faster than other forms of membrane fusion. The synaptic vesicle protein Synaptophysin forms hexamers which bear 2 copies of the v-SNARE VAMP at each vertex, one likely assembling into a peripheral SNAREpin and the other into a central SNAREpin.

Keywords

Neurotransmitter release, intra-vesicular pressure, SNAREpins, Munc13, Synaptophysin

Abbreviations

CryoEM – cryo-electron microscopy, DAG – diacylglycerol, GUV – giant unilamellar vesicles, NSF - N-ethylmaleimide sensitive factor, PM – plasma membrane, SNAP – synaptosomal-associated protein, SNARE - soluble N-ethylmaleimide-sensitive-factor attachment protein receptor, pSNAREpins – peripheral SNAREpins, cSNARE

pins – central SNAREpins, v-SNARE – vesicular SNARE, t-SNARE – target SNARE, SUV – small unilamellar vesicles, SV – synaptic vesicle, Syt1 -Synaptotagmin 1, TIRF - Total internal reflection fluorescence mircroscopy, VAMP2 – vesicle associated membrane protein 2.

Introduction

The core machinery of neurotransmitter release is well-known [1] but how this machinery choreographs ultra-fast synaptic transmission is still veiled in mystery for lack of understanding of the supra-molecular structures responsible. Six years ago, we proposed a then-speculative model [2] to explain how individual SNAREs are clamped and co-operatively released in the context of a symmetrical ring-like assembly at the terminal stage of "ready-release" synaptic vesicles (Fig. 1). This "buttressed rings hypothesis" was originally motivated largely by geometric considerations. The idea for an inner ring of Synaptotagmin came from the unexpected discovery that isolated Synaptotagmin self-assembles into Ca^{++}-sensitive rings of ~15-20 subunits on lipid monolayers and into similar diameter tubules budding from lipid bilayer vesicles, driven by self-association of its Ca^{++} and PIP_2-binding C_2B domain [3, 4].

The idea for the outer ring came from the shape of the Munc13 protein, already well-recognized to be both a Synaptic Vesicle (SV) tether and a key SNARE complex assembly chaperone [5, 6]. Unlike other flexible vesicle tethers, Munc13 was noted to possess a rigid "banana-like" shape which we more specifically noticed would represent ~60^o of arc when it lies flat on a membrane, suggesting how a symmetrical arrangement into a ring would limit the number of SNAREpins that could be assembled under each SV to a total of 6 (Fig. 1A).

Then, taking into account the detailed geometry of binding of Synaptotagmin to a SNAREpin from X-ray crystallography [7, 8], we suggested that SNAREpins could maximally occupy every 3^{rd} position of an Synaptotagmin ring without sterically clashing (Fig. 1D). This in turn implied that the proposed 6 SNAREpins would require an inner ring of ~18 Synaptotagmins, which fit closely within the proposed outer ring of 6 copies of Munc13 (Fig. 1D). The inner ring of Synaptotagmin is predicted to restrain the 6 SNAREpins from fusing in its Ca^{++}-free state, but then synchronously release them to fuse when it binds Ca^{++}. The ring dissociates because the same interface that is used to form the ring is also used to interface with the bilayer, and both cannot happen at the same time [3].

Many of these predictions have since been tested, and important new structural and functional information has appeared, motivating us here to re-visit and amplify the model especially as it concerns the likely structures that govern the

earlier stages in vesicle capture and maturation into ready-release vesicles which could not be addressed in 2017.

Structural and functional evidence for the Synaptotagmin ring

Cryo-EM tomography analysis of SV docked to the plasma membrane (PM) of NGF-differentiated pheochromocytoma (PC12) cells [9] revealed a symmetric circular arrangement of rod-like protein densities between the vesicle and the membrane, consisting of 6 "exocytosis modules" arranged as if on a ring of ~35 nm outer diameter, as predicted by the buttressed rings hypothesis. The size of the resolved portion of each module was most consistent with a single SNAREpin and associated chaperones. We observed the same arrangement of 6 densities in synapses in hippocampal neuronal cultures, with clear separation of the SV and PM bilayers, separated from the contact point by ~3 nm [10]. The predicted Munc13 and Synaptotagmin rings could not be visualized, as would be expected given the limited resolution (~4.4 nm) and their close apposition to the PM bilayer.

Nonetheless, rings containing Synaptotagmin can be inferred through the structural and functional effects of a structure-based mutation (F349A) in the contact surface that disrupts ring assembly by the isolated protein without affecting SNARE binding, Ca^{++}-binding or acidic lipid binding [11]. This mutation completely disrupts the symmetric ring organization [9] as well as SV exocytosis in undifferentiated PC12 cells, increasing spontaneous release so dramatically that it occludes evoked release [11].

Synaptotagmin oligomers are also necessary and sufficient to form a Ca^{++}-sensitive fusion clamp in a simplified *in vitro* system [12-14] which monitors the fate of single vesicles docking to a suspended bilayer. Each vesicle contains ~10-15 copies of externally-oriented VAMP and ~25 copies of externally-oriented Synaptotagmin to mimic SV. The bilayer contains pre-assembled Syntaxin-SNAP25 t-SNAREs, thereby bypassing the need for Munc18 and Munc13 chaperones. Under these conditions, Synaptotagmin is the only potential source of a fusion clamp. The vesicles stably dock to the bilayer in the absence of Ca^{++}, and then efficiently release their content in ≤10 msec (measurement limited by optical time resolution) after exposure to 100 µM Ca^{++}[14]. As it takes ~1 sec half-time after docking for vesicles containing only VAMP v-SNAREs to spontaneously (and asynchronously) fuse [15], Synaptotagmin is evidently sufficient both to

synchronize and speed up release by at least 100-fold. As predicted from our hypothesis, destabilizing the Syt1 oligomers with the F349A mutation then results in spontaneous fusion of ~ 85% of the docked vesicles in the absence of Ca^{++} [15].

When the vesicles contain only 5-10 externally-oriented copies of VAMP the number of SNAREpins in each docked ready-release vesicle is ~6±2 [16]. With larger numbers of copies of VAMP, more representative of natural SVs (which contain ~70 copies [17]) the number of SNAREpins per vesicle is much greater and much more variable, ranging from 5-35 [16] and it becomes necessary to clamp the additional SNAREpins with a second complementary, Synaptotagmin-independent clamping mechanism involving Complexin [15]. Now, as expected, even vesicles containing F349A Synaptotagmin remain stably docked to the bilayer; however, they can no longer be released by Ca^{++} because they are arrested by Complexin and not the Ca^{++}-sensor Synaptotagmin [15]. As we discuss in the next sections, the deeper explanation is that Synaptotagmin and Complexin are normally working in tandem clamping two distinct populations of SNAREpins.

As would be expected given that there are multiple mechanisms of clamping, the effects of F349A, while clear, are buffered in neurons [18] suggesting that other stabilizing interactions are present in more tightly regulated neuronal synapses. Using a combination of fluorescence imaging and electrophysiology of individual boutons (whose behavior varies widely) in neocortical synapses, we found that Synaptotagmin F349A increases all forms of release: spontaneous, synchronous, and asynchronous, the extent varying greatly from bouton to bouton.

Söllner, Briggs and colleagues [51] used cryo-EM tomography to quantitatively characterize the organization of protein densities at the interface of Ca^{++}-releasable small unilamellar vesicles (SUVs) docked to giant unilamellar vesicles (GUVs) formed in a simplified reconstitution containing VAMP2 and Syt (SUV) and Munc18-Syntaxin (GUV) along with SNAP25 and Complexin. They found that the structures observed depended critically upon inter-bilayer separation, but that at the smallest separations (<3 nm) only ring-like arrangements were observed. Though they could not specifically identify the complete and partial rings as containing Syt due to limited resolution, the dimensions observed were consistent with the results obtained with self-assembling isolated Syt [3,4]. A more recent follow-up study by Chapman and colleagues [19] measuring average changes in populations of boutons confirmed that Synaptotagmin oligomerization is a

primary mechanism for clamping and provided novel evidence that the juxta-membrane linker region contributes to oligomerization.

How can simultaneous release of a handful of SNAREpins from the Synaptotagmin ring accelerate fusion pore opening by at least 100-fold? The explanation appears to be *mechanical coupling* - though seemingly independent, SNAREpins are in fact mechanically coupled by virtue of sharing common bilayers. Though we typically think of membranes as quite fluid and flexible, which they are on the micron scale, they are extremely rigid on the nanoscale of an ~10 nm SNAREpin [20]. Quantitative physical modeling based on empirical parameters incorporating this simple idea results in the remarkable prediction that sub-millisecond initial fusion pore opening can result from 3 – 6 synchronously released SNAREpins over a wide range of parameters [20]. Real-time measurement of single fusion pores from single vesicles fusing with suspended bilayers confirm that a stable fusion pore opens whenever 3 or more SNAREpins simultaneously zipper [21] consistent with a large body of earlier work using less direct methods.

In summary, evidence from biochemistry, genetics, and electron microscopy demonstrates the predicted 6-fold symmetric organization of the SV-PM interface and strongly supports the idea that a ring of Synaptotagmin contributes importantly to clamping and release of synaptic vesicles for synchronous neurotransmission. Proof will require directly visualizing the rings and their structure at high resolution. Modeling and direct experiments demonstrate that zippering of as few as 3 synchronously-released SNAREpins can result in ultra-fast opening of fusion pores.

<u>Peripheral vs Central SNAREpins</u>

Two functionally distinct populations of SNAREpins can be operationally distinguished in the docked ready-release vesicles that are synergistically clamped *in vitro* by Synaptotagmin and Complexin. We term them ‘peripheral’ SNAREpins (pSNAREpins) and ‘central’ SNAREpins [15] (cSNAREpins). All cSNAREpins are clamped by direct binding to Synaptotagmin, and they are directly released by Ca^{++}. pSNAREpins are directly clamped by Complexin and indirectly by Synaptotagmin.

Several otherwise perplexing observations are easily explained by this model:

1. Vesicles lacking Synaptotagmin are clamped by Complexin alone (when docking is artificially delayed) but then cannot be released by Ca^{++}. As noted, in the absence of Complexin vesicles are efficiently clamped by Synaptotagmin when they contain only 5-10 outward facing copies of VAMP and therefore a limited number of SNAREpins, measured to be 6±2 (central) SNAREpins [16]. When they contain an excess of ~10-15 copies of VAMP now additional (peripheral) SNAREpins can form, and these pSNAREpins require Complexin to be clamped.

2. Selectively removing Complexin (by dilution) triggers immediate fusion [15] because it liberates the pSNAREs. But doing so in the presence of excess soluble t-SNAREs (the 1:1 complex of SNAP25 with the cytoplasmic domain of Syntaxin, which sequesters the VAMPs involved in pSNAREpins to prevent them from driving fusion) retains the Synaptotagmin-cSNAREpin clamp, thus enabling Ca^{++} - triggered release by remaining cSNAREpins (which presumably are more stable due to Synaptotagmin binding and to steric protection by the Synaptotagmin ring).

3. SNAREpins assemble in two distinct and equal waves, separated by a lag phase of ~0.5 sec [16]. When ring assembly is prevented (F349A mutation) this pronounced lag is eliminated. Now SNAREpins assemble much more slowly overall and in a single bolus. This suggests that the ring together with one set of directly bound SNAREpins co-operatively co-assembles, and that a second and distinct set of SNAREpins can only begin its assembly after that.

Given these properties, the cSNAREpins are expected to be positioned on the Synaptotagmin ring, consistent with the fact that primary site binding between C_2B, SNAP25, and Syntaxin [7, 8] is required for them to clamp [15]. Note that a second copy of Synaptotagmin is thought to bind to a “tripartite” site on the opposite side of the SNAREpin [8] an interaction whose relevance has been called into question [22]. While this tripartite interaction is compatible with our models [2] it is not a necessary feature.

How, then, are the peripheral SNAREpins arranged under the docked vesicle, if they are not bound to Synaptotagmin? We previously discovered [23] a specific pair-wise relationship between “*trans*-clamped” SNAREpins in a crystal of half-

zippered SNARE complexes which are linked somewhat anti-parallel to each other by a bridging molecule of Complexin (Fig. 2A). The bridging Complexin is bound to the outside of one SNARE complex by its central helix, where it branches away from the body of the helical bundle by ~45 degrees, terminating in its accessary helix, which then binds into the groove of the paired t-SNARE complex in place of the C-terminal half of its own VAMP v-SNARE (which was not present). Both the trans-interaction (K_d ~15 μM) and the unusual, branched conformation were independently demonstrated in solution [23].

Although our original interpretation [23] was based on the zig-zag array that was a feature of the crystal packing and is no longer relevant, we suggest that the trans-interaction between SNAREs is quite relevant, both because it has been validated in solution [24] and is supported by extensive genetic evidence confirming that numerous modifications of the accessory helix increase or decrease the rate of spontaneous release in mice, flies, and worms [25-27]. Further, these very accessory helix mutations correspondingly disrupt the clamping of pSNAREs by Complexin in the reconstitution [14]. The Complexin accessory helix also can interact with the membrane-proximal portions of VAMP2 and SNAP25 based on cross-linking [28].

Altogether, this naturally suggests that pSNAREpins and cSNAREpins are trans-clamped by a bridging molecule of Complexin as pairs under each ready-release vesicle, in the manner of the crystal structure. When this Complexin is removed (by dilution) the pSNAREpins are selectively released to trigger fusion independent of Ca^{++}. Normally, when the Complexin is retained, the appearance of Ca^{++} directly releases the cSNAREpins as the Synaptotagmin ring dissociates. This radical change in geometry would simultaneously remove the accessory helix (emanating from each cSNAREpin) from the pSNAREpins, thereby indirectly releasing them at the same moment. Ca^{++} therefore releases all the SNAREpins simultaneously in this model.

Satisfyingly, the trans-clamped arrangement of paired SNAREpins observed in crystals fits readily and naturally into the framework of buttressed rings model [14]. In Fig. 2B we have simply added a second (peripheral) SNAREpin to each central SNAREpin according to the trans-clamped structure (Fig. 2A). The result is that the cSNAREpins are bound to the inner Synaptotagmin ring while the pSNAREpins are not; they project radially and upward (with C-terminal end

oriented down), roughly paralleling the SV surface (Fig. 2B and 2C). Note that this positioning is not exact and is likely to vary with the extent of zippering beyond the X-ray structure [22]. Each pair is linked by a Complexin accessory helix binding to the pSNAREpin whose central helix is bound to the cSNAREpin. This proposed paired arrangement of peripheral and central SNAREpins implies that they will always be equal in number and that two closely located molecules of VAMP are needed to form each pair, predictions that will be discussed next in connection with the VAMP-binding SV protein Synaptophysin.

In summary, we suggest there are equal numbers of peripheral and central SNAREpins. The 6 central SNAREpins are directly bound to the inner Synaptotagmin ring, are directly released by Ca^{++}, and they initially open the fusion pore. The 6 peripheral SNAREpins are indirectly bound to the ring, each linked to a central SNAREpin by a bridging molecule of Complexin.

Counting SNAREpins and Synaptophysin

Testing these predictions *in vivo* is beyond current capabilities. However, it is possible to directly count the number of SNAREpins associated with each ready-release vesicle in the reconstituted vesicle-bilayer fusion system using well-established single molecule methods involving TIRF. We employed a variation of the suspended bilayer chip [12] specially adapted to enable TIRF imaging [29] thereby allowing single-molecule counting by step-photobleaching of SNAREpins labelled with fluorescent Complexin [16].

VAMP has long been known to form complexes with Synaptophysin [30, 31] the most abundant SV membrane protein by mass [17]. Stowell and colleagues [32] more recently reported that Synaptophysin can assemble into hexamers, and that each such complex can bind up to 12 copies of the v-SNARE VAMP. Based on this, they suggested that Synaptophysin would both template a ring-like arrangement of 12 SNAREpins and accelerate their rate of assembly.

As previously mentioned, when physio- mimetic numbers of VAMPs (~70) are present in each vesicle, the number of resulting SNAREpins per vesicle varied widely, from as few as 5 to as much as 35, increasing in rough proportion to vesicle diameter [16]. As predicted by Adams et al [32], adding Synaptophysin to the vesicles dramatically changes the result. Now all docked vesicles have just 12

± 1 per vesicle, independent of their size [16]. Moreover, the rate of SNAREpin assembly was greatly accelerated by Synaptophysin. This provides the direct evidence that hexameric complexes of Synaptophysin and VAMP dimers exist in lipid bilayers (as distinct from detergent extracts) and function as a specialized chaperone that templates 12 SNAREpins per vesicle. In principle, these 12 SNAREpins could be arranged symmetrically and equivalently as suggested [33]. However, we now know this is not the case when Synaptotagmin and Complexin are present, as the 6 central SNAREpins (clamped by Synaptotagmin) and the 6 peripheral SNAREpins (clamped by Complexin) are by virtue of these properties non-equivalent.

Synaptophysin is a member of the tetraspanin protein family which consists of Synaptophysin, Synaptoporin, and Synaptogyrins1–4, among others [34]. From a genetics point of view the evidence over the past 20 years strongly suggests that tetraspanins are not critical for proper synaptic function [35, 36]. Our model can explain this since so much of the SNARE organization is going to be set by the Synaptotagmin ring and Munc13 oligomers and the geometrical constraints they impose, as we will now discuss.

In summary, Synaptophysin hexamers likely provide a key driving force to template the observed overall 6-fold symmetry at the SV-PM interface. Two copies of the v-SNARE VAMP emanate from each vertex, one assembling into a peripheral SNAREpin linking to a paired central SNAREpin.

Distinct oligomers of Munc13 likely assemble peripheral and central SNAREpins

The core functional C-terminal portion of Munc13 (Munc13C, consisting of its C_1–C_2B–MUN–C_2C domains) spontaneously assembles with phosphatidylserine-rich vesicles to form an extensive two-dimensional protein crystal sandwiched between two planar bilayers. Within this crystal Munc13 is organized into two distinct oligomeric assemblies, each having a distinct molecular conformation [37]. In its ‘open’ molecular conformation, Munc13 forms upright trimers that link the two bilayers, separating them by ∼21 nm (Fig. 3A). In its ‘closed’ molecular conformation, 6 copies of Munc13C interact to form a lateral hexamer elevated ∼14 nm above the bilayer (Fig. 3B). Open and closed conformations differ only by a rigid body rotation around a flexible hinge, which, when performed cooperatively, transitions Munc13 from the upright trimer into the lateral

hexamer (Fig. 3C and see Movie S2 https://www.pnas.org/doi/abs/10.1073/pnas.2121259119#supplementary-materials). We suggested (Fig. 4) that the assembly of trimers (state 1) and hexamers (state 2) may represent two successive states in the synaptic vesicle supply chain leading to "primed" ready-release vesicles in which SNAREpins are clamped and ready to release (state 3). A recent cryo-EM tomography study [38] reported that Munc13 and SNAP25 are needed for SV localization, respectively, to ~10 nm and ~5 nm from the PM, likely corresponding to our proposed states 2 and 3 respectively, and that DAG may promote this transition.

The lateral hexamers are formed by unique asymmetric contacts between the C_2C of one copy of Munc13 and the MUN domain of its neighbor in the hexagon ring. These contacts block access to the site on Munc13 needed to open the closed Munc18-Syntaxin complex to initiate SNARE complex assembly [5, 39, 40]. For this reason, we proposed [37] that SNAREpin assembly by Munc13 is autoinhibited in the lateral hexamer by the neighboring copy of Munc13.

To test whether these novel crystal structures could be functionally relevant for SNAREpin assembly and for fusion, we mutated conserved amino acids at both surfaces engaged in unique subunit contacts. Consistent with this [41] such mutations in the unique contacts defining the trimer and hexamer interfaces disrupted the corresponding oligomer within crystals, profoundly reduced synaptic function in *C. elegans* and resulted in docked vesicles produced *in vitro* that failed to be released by Ca^{++} which had few if any detectable SNAREpins, employing a complete reconstitution that is Munc13- and DAG-dependent [42].

In summary, distinct Munc13 trimeric and hexameric oligomers co-operate in assembling SNAREpins. We suggest that the trimers lead to assembly of the 6 peripheral SNAREpins and that the hexamers, which position the SV closer to the PM, lead to the later assembly of the 6 central SNAREpins.

Inter-membrane separation likely governs SNAREpin assembly during transitions between Munc13 oligomeric assemblies

While the genetic and biochemical validation of upright trimers and lateral hexagons of Munc13 provides an overall framework for understanding how ready-release vesicles are assembled (Fig. 4) it also poses new questions

concerning how the transitions between oligomeric assemblies occur and their relationship to SNAREpin assembly.

There are strong physical constraints that determine when SNAREpins can assemble, and indeed it has been observed that the arrangements of protein densities in reconstituted synaptic systems depends critically upon inter-bilayer separation [51]. Can the Munc18-VAMP-Syntaxin template complex, a key intermediate in SNARE complex assembly, form in State 1 or State 2 (Fig. 4) given the inter-membrane separations involved? The Munc18-VAMP-Syntaxin template complex needed for concerted assembly of SNAREpins can appreciably exist only when z < 11-12 nm [43, 44][1]. For comparison, z= 21 nm for a SV bound by a single upright trimer (Fig. 3A) and z = 18 nm when bound by 6 upright trimers simultaneously (State 1; Fig. 7A) both well out of range for template complexes to form. On the other hand, z= 12 nm at the closest possible approach atop a lateral hexamer (State 2; Fig 3B), within range given the various uncertainties in the estimates involving the template complex, our model, and thermal fluctuations. We conclude that chaperoned SNARE assembly is not possible in State 1 but can occur in State 2.

What about the product of the template complex, partially zippered SNAREpins – will they be stable once produced in State 2? Modeling experiments (Fig. 7) taking into account the constraints of both VAMP binding at Synaptophysin vertices at the SV and SNAP25 palmitoylated loop binding to the PM reveal that partially zippered SNAREpins are sterically permitted in numerous arrangements, certainly in State 2 but even in State 1. In State 1 the four-helix bundle can be zippered as far as layer -1, and it can be zippered up to layer +4 in State 2. Both of these potential SNAREpin geometries are likely to be stable. For example, the most N-terminal portion of VAMP (which initiates zippering) spontaneously assembles within the context of the full-length protein into a transient ~5 turn α-helix (termed helix I, extending from residues 36-54) thought to nucleate the v-SNARE zippering process [45], and an overlapping peptide (residues 28-47) binds to

[1] The maximum membrane separation that permits template complex formation can be estimated as the sum of the size of the folded template complex along the pulling direction (5.8 nm from the structure of the template complex [44]) and the extensions of the unfolded Syntaxin and VAMP2 (total 40 amino acid residues). While the latter is strongly force-dependent, the template complex can only sustain a limited force: an equilibrium force of 5.1 pN or an estimated maximum force of 6.5 pN (Fig. 3C in [43]. Bracketed by these two forces, the maximum membrane distance will then be between 11 and 12 nm. We thank Professor Yongli Zhang (Yale) for making this estimate.

Syntaxin-SNAP25 with K_d ~10 µM [46]. The former would represent zippering to layer -1 and the latter to layer -3 [47].

In summary, the conclusion from biophysical considerations is that SNAREpin assembly will be limited by the stability of the molecular chaperone template complex rather than the inherent stability of the resulting SNAREpins. The former is ultra-sensitive to inter-membrane separation; the latter is not. This allows chaperoned assembly of SNAREpins in State 2 but not in State 1 (Fig. 4).

Diacylglycerol- and Ca^{++} likely govern the oligomeric transitions of Munc13 and thereby choreograph the assembly of peripheral SNAREpins, central SNAREpins, and the buttressed rings

Important for this speculative discussion is the further hexagonal organization of upright trimers (Fig. 5A, showing a slice of the structure at the level of the SV) that exists in the crystal (but which has not yet been validated through evidence independent of the crystal). Specifically, an upright trimer is at every vertex and two Munc13 subunits of neighboring trimers contact each other to form the sides of the hexagon, which contains 18 copies of Munc13 altogether [37]. More specifically, the sides are formed by oppositely oriented diacylglycerol (DAG)-binding C_1 domains emanating from neighboring trimers near the PM (Fig. 5C). An important feature of the structure is that C_1 domains in the open molecular conformation found in the upright trimer are sterically prevented from binding DAG because the binding site faces perpendicularly away from the surface of the PM and is elevated well above it (Fig. 6A). However, in the later closed conformation of the lateral hexamer the DAG-binding surface is now rotated into direct contact with the PM surface (Fig. 6B) enabling them to bind DAG.

Though the three subunits of an isolated trimer are structurally equivalent, they become non-equivalent when the trimers further organize into an 18-mer hexagon. For example, when an SV binds at the center it can contact the C_2C domain of only one subunit of each trimer (labeled 'Inner' in Fig 5A). Also, a unique subunit of the trimer at each vertex has an unpaired C_1 domain, pointing approximately radially outward at the PM level (arrows in Fig. 5B). Tracing up from the PM level (Fig. 5B) towards the SV level (Fig. 5A) reveals that the 'Medial' (non-SV contacting) copy of Munc13 bears the uncombined C_1 domain. In particular, we expect that DAGs will bind to the Medial Munc13s before they can

bind to Inner or Outer Munc13s because these C_1 domains are involved in a separate interaction which must first be disrupted.

The proposal that DAG binding initially occurs at the 6 Medial Munc13s while the SV is retained by the 6 Inner Munc13s has interesting consequences. When the Medial copy of Munc13 is stabilized in the closed conformation by binding DAG, it will concomitantly be removed from the trimer (Figs. 3C and 7A), destabilizing the remaining Outer and Inner copies which then also dissociate. The Inner SV-contacting copies of Munc13 can remain with the SV, forming a flexible, wobbly stool with 6 now-flexible legs (Fig. 7A). Each leg consists of a rigid body of C_1-MUN-C_2C attached by a flexible linker to a fixed base of C_2B at the PM [37]. In addition, the C_2C domains can now slide around on the SV surface while still remaining attached to the bilayer. Together, the removal of these constraints should allow major fluctuations of inter-membrane separation (z) that are not possible with Munc13 trimers where z is rigidly either 18 or 21 nm.

When the SV fluctuates to z < 11-12 nm template complexes will form, and if Munc13 and SNAP25 are available these can be assembled into SNAREpins. The now-released formerly Medial and Outer copies of Munc13 (which should both now have bound DAG and therefore be free to assemble SNAREpins in their more PM-proximal closed conformations) should create a permissive environment for SNAREpin assembly in which both the Munc18 template complex and Munc13-SNAP25 complexes [48] are locally available.

The maximum number of SNAREpins that can form at this stage is 12, limited by the Syp_6-$VAMP_{12}$ complex (Fig. 1C). In that case, why would only 6 pSNAREpins be assembled at this stage? The simplest possibility is that only 1 SNAREpin can sterically be accommodated between the legs of the 6 surrounding MUN domains either in State 1 (Fig. 7B) or in State 2 (Fig. S1). Another possibility (Fig. 7B) is that for currently unknown reasons only one of the two copies of VAMP at each vertex of Synaptophysin is sterically accessible in Stages 1 and 2, but becomes available during the transition to Stage 3. In line with this, the SNARE motif of VAMP is known to interact with the cytoplasmic C-terminal domain of Synaptophysin [49] and prevents assembly with t-SNAREs [30, 31]. In either case, we suggest that one copy of VAMP at each vertex of the Synaptophysin hexagon remains free for later assembly of the central SNAREpins.

Once nucleated, zippering of the pSNAREpins should serve as a driving force to push the SV ever-closer to the PM, making all subsequent steps in SV priming effectively irreversible. For example, pSNAREpins will stabilize State 2 by forcing the SV against the top of the lateral hexamer of Munc13 toward the PM. Importantly, pSNAREpins will be clamped from further zippering by the integrity of the lateral hexagon structure. This would serve to create a readily mobilized reserve pool of SVs as has been observed in physiologic studies [50, 51]. The purpose of this reserve pool is to replace "primed" ready-release SVs (State 3 in Fig. 4) that are released by the same wave of Ca^{++}. In our model [37] this occurs when Ca^{++} binds to the C_2B domains at the PM-attached feet of the Munc13 lateral hexagon. Analogous to the corresponding power stroke of Synaptotagmin's Ca^{++}-sensing C_2B domain [52] this is thought to trigger aliphatic loop insertion into the PM and rotation of Munc13's C_2B. This motion will collapse the lateral hexamer as the C_2B-attached MUN domains rotate the MUN domains onto the PM.

Critically, this same motion would simultaneously remove the autoinhibiting C_2C domains from the neighboring MUN domains in the lateral hexamer, now allowing further (central) SNAREpin assembly to proceed from the remaining 6 VAMPs bound to the vertices of the Synaptophysin hexagon [36]. Though there is as yet no insight into the resulting structure, we suggest in general terms that the 6 central SNAREpins are coordinately assembled when the lateral hexamer disassembles and its subunits now re-arrange to form the outer Munc13 ring of the ready-release vesicle originally envisioned in the buttressed rings model [2]. The peripheral SNAREpins would further zipper during the transition to State 3 (Fig. 4) and provide driving force to make this transition irreversible (Fig. 2B).

The inner Synaptotagmin ring needs to be ready during the transition to State 3 to receive and clamp the newly-made central SNAREpins[2]. Critically, assembly of the Syt ring (~ 25nm diameter at its C_2B domains) will be sterically prevented by the presence in State 2 of the lateral Munc13 hexagon (~ 16 nm diameter at its C_2B domains) which occupies the same PM surface.

[2] While there are compelling reasons to suggest that Munc13 assembles pSNAREpins before cSNAREpins, it is possible that when Munc13 is artificially using pre-assembled t-SNAREs that this order is reversed.

It is therefore likely that the inner ring, the outer ring, and the central SNAREpins all form in a tightly coupled process in which the 6 Munc13s comprising the lateral hexagon move outward and flatten to form the proposed outer ring of MUN domains (Fig. 1B) and allow the inner ring of Syt to assemble in a concerted fashion. It is then easy to imagine how the previously-assembled peripheral and the just-assembled central SNAREpins would concomitantly pair up locally by Complexin. Further zippering of the 6 peripheral SNAREpins would be prevented by the mechanical impediment of the enclosed Syt ring and by trans-clamping, while further zippering of the 6 central SNAREpins would be prevented by their radial retention on the Syt ring. All 12 SNAREpins would be synchronously released by Ca^{++} binding.

In summary, we suggest that peripheral SNAREpins are assembled before central SNAREpins. We suggest that synaptic vesicles are captured by an 18-mer hexamer of upright Munc13 trimers. DAG binding then initiates disassembly of these 'open' conformation trimers and the assembly of the 6 vesicle-contacting copies of Munc13 into a 'closed' conformation lateral hexamer. The 6 peripheral SNAREpins are assembled during this transition, and help drive it, and the result is a population of easily mobilized but still unprimed reserve vesicles. Ca^{++} triggers the auto-inhibited lateral hexagon beneath the reserve vesicle to rearrange to form the outer ring of 6 copies of Munc13 while simultaneously assembling the 6 central SNAREpins and allowing the inner ring of Synaptotagmin to form and clamp these SNAREpins in place. The inner ring of Synaptotagmin is sterically unable to assemble until the lateral hexamer of Munc13 first disassembles. The overall result is transition of the reserve vesicle into a primed, ready-release vesicle. These molecular steps could underly the sequential two-step priming scheme that has been proposed by Neher and colleagues to explain a variety of physiological observations [51, 53].

<u>Peripheral SNAREs may 'turbocharge' synaptic vesicle release</u>

In addition to their likely role in providing energy to drive the overall process of vesicle docking forward, pushing the vesicle ever-closer to the plasma membrane, peripheral SNAREpins can potentially accelerate fusion pore opening and neurotransmitter release by *turbocharging* the engine of central SNAREpins. *Turbochargers* improve the performance of an engine by adding a boost of additional pressure.

It is strongly predicted that pSNAREpins will accelerate neurotransmitter release, even after the fusion pore first opens. This is because pSNAREpins will necessarily complete their zippering after cSNAREpins as the direct consequence of their more peripheral radial locations. When SNAREpins complete zippering they no longer exert force, so it follows from this first principle that pSNAREpins will continue to exert force even after the cSNAREpins have fully zippered at which point the fusion pore must already have opened.

There are at least three synergistic mechanisms by which force-generating pSNAREs could turbocharge the overall process of release, by 1) accelerating terminal zippering of the cSNAREpins to open the fusion pore faster; 2) accelerating expansion of the fusion pore; and 3) accelerating release of the neurotransmitter through the open fusion pore.

1. Turbocharging pore opening. Terminal zippering of SNAREpins between two bilayers differs energetically from zippering of isolated SNARE complexes in that work is required to bring the two bilayers together, ever more so as the bilayers get closer and closer. Steric repulsion must be overcome, layers of bound water must be removed, and ultimately the surface of the phospholipid bilayer must be disrupted. Zippering against such a load will be accelerated by applied forces that synergize to lift the load, which we suggest in general terms peripheral SNAREpins will do. More specifically, the energy landscape of zippering SNAREpins contains several pause points, local hills and valleys corresponding to activation energy barriers that populate intermediate zippering states to facilitate regulation [54]. Adding pSNAREpins will potently counter these loads by providing more pulling force and reducing the height of the barriers in the energy landscape. For example, a reduction of only 5 k_BT will accelerate zippering across such a barrier by a factor of ~150-fold. Since each pSNAREpin can add up to 60 k_BT, it is easy to see how the interval between release of cSNAREpins and the initial opening of the fusion pore could be considerably accelerated by pSNAREpins.

2. Forced expulsion of neurotransmitter thru the fusion pore. Neurotransmitters are generally assumed to exit thru the opening fusion pore by simple diffusion. Models of this process suggest that ~90% of neurotransmitter will diffuse out in ~ 2 msec (See supplementary Text). However, because of peripheral SNAREs a new possibility exists, namely that forces from these SNAREs continuing after fusion pore opening will create positive pressure within the vesicle that actively propels

the transmitter out thru the pore (Fig. 8A). The pSNAREpins flatten and pressurize the primed vesicle by pulling on the membrane at a radial distance of d ~10 nm from the contact point. We estimate that the pressure inside the vesicle can reach ~2 atm. A simple model predicts release in ~500 µs under the action of the pressure induced by the peripheral SNAREpins (See Supplementary Text and Supplementary Fig. S4).

3. Turbocharging fusion pore expansion. The pressure gradient created by pSNAREs (inside > outside vesicle) will extend into the fusion pore, pushing its wall radially outward, expanding the pore diameter (Fig. 8B). The result is that pore expansion is predicted to be dramatically faster with pSNAREpins than with cSNAREpins alone. A simple model suggests that the fusion pore can reach a diameter of ~10 nm in ~200 µs because of the pressure generated by pSNAREpins vs ~1.5 nm with cSNAREpins alone (see Supplementary Text and Supplementary Fig. S3).

Peripheral SNAREpins could also provide a biochemical basis for the proposed reversible tightly docked state of SVs [53], as the exposed pSNAREpins (but not the sequestered cSNAREpins) would likely be more susceptible to ATP-dependent dissociation mediated by NSF and SNAP.

In summary, forces that continue to be exerted by peripheral SNAREpins, even after central SNAREpins have already opened a fusion pore, will likely reduce the delay between vesicle unclamping and complete neurotransmitter release at many stages of this process.

Perspectives

The updated buttressed ring model answers some questions but of course raises many more. The first glimmer of evidence for the model was the predicted 6-fold symmetry revealed by cryo-EM tomography at very modest resolution [8,9]. We now refine this interpretation by suggesting that each of the 6 observed densities correspond to the resolvable portion of an exocytosis module which consists of not one (our original interpretation) but rather two SNAREpins.

One of these, the central SNAREpin, was the core of the original model; new data have caused us to incorporate a second, peripheral SNAREpin into this unit, which

most likely is not resolved. The discovery of pSNAREpins from cell-free functional assays and their postulated roles in turbocharging neurotransmitter release can help illuminate the long-standing question of how ultra-fast synaptic transmission can be achieved using ordinary fusion machinery.

New insights into Munc13 oligomeric assemblies hint at a very sophisticated choreography of vesicle to membrane in which increasing potential energy is stored in successively smaller volumes as Munc13 ratchets the vesicle toward the membrane, allowing an explosive process of release. It seems likely that the four repeat domains within the MUN domain are capable of interacting with each other in multiple ways to program these movements, in ratchet-like steps that bring the vesicle ever-closer to the membrane.

Assembly of the inner Synaptotagmin ring must be tightly linked to the assembly of the central SNAREpins, but how this happens is unclear. It is clear, however, that there is no room within the lateral hexagon of Munc13 to accommodate the ~18 copies of Synaptotagmin needed to form the inner ring, so there must be some sort of concerted inward movement of the Synaptotagmin coupled to an outward movement of the 6 copies of Munc13 comprising the lateral hexagon as they flatten onto the plasma membrane. In the process of this pivotal event, the inner (Synaptotagmin) ring and outer (Munc13) rings somehow coordinately assemble, and the 6 central SNAREpins are assembled and are placed symmetrically on the inner ring as Munc13 and Munc18 complete their duty cycles. Peripheral and central SNAREpins lock in place by trans-clamping and a primed, ready-release vesicle is formed. The details are far from being clear, as are the precise roles of the peripheral SNAREpins in fusion pore opening and dynamics.

Testing the model and its many structural and functional predictions will ultimately require new methods to capture a series of sequential and rather large structures self-assembling between membranes, representing stages in the docking, priming, and release process. Such high resolution cryo-EM structures will need to be combined with functional assays and key genetic/physiological tests.

It would appear that the relevant assemblies will have as many as 108 polypeptide chains (12 copies each of VAMP, SNAP25, Syntaxin, Munc18, and

Complexin; 24 copies of Synaptotagmin -18 in the inner ring binding via the primary site, and 6 binding via the tripartite site [8]-; 6 copies of Synaptophysin; and 18 copies of Munc13), considering just the main known components. The total mass of these proteins would be about 3.5 million Daltons, roughly equivalent to two E. coli ribosomes, and at its largest would occupy a volume similar to three ribosomes. Fortunately, these structures are likely to have a high degree of symmetry, but producing and solving them will be a major challenge.

Acknowledgements
We thank Jeremy Dittman, Shyam Krishnakumar, and Kirill Volynski for their helpful comments on the manuscript. We also thank Yongli Zhang for his calculations concerning the template complex.

Figures.

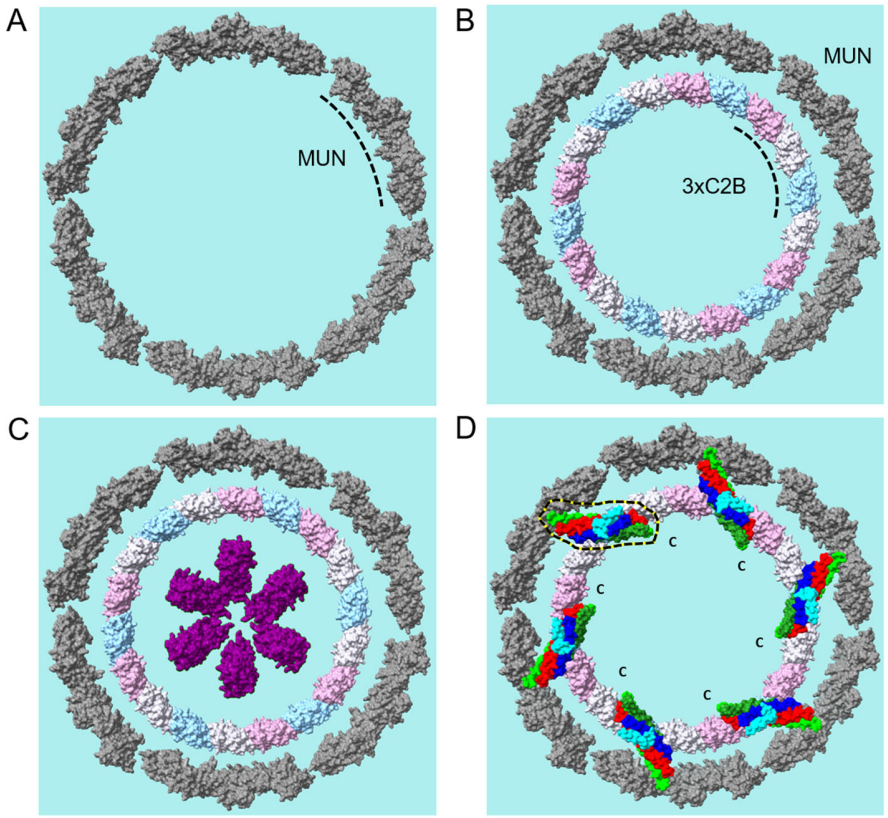

Figure 1. The original buttressed rings model. Concentric rings of the SNARE assembly chaperone Munc13, the Ca^{++} sensor Synaptotagmin (Syt), the v-SNARE chaperone Synaptophysin (Syp) as seen from above the PM. Working together with other proteins, the concentric rings are suggested to enable co-operative SNARE clamping and Ca^{++}-triggered release. (A) Six MUN domains (grey) of Munc13 molecules are hypothetically arranged in an end-to-end manner on the PM to form a flat ring-like structure with an inner diameter of ~26 nm. The black dashed arc line denotes one such Mun domain. (B) The hypothetical 6 member Munc13 ring could tightly encircle a concentric Syt1 ring consisting of 18 C2B domains. Each Munc13 molecule would cover ~21 nm arc length on the membrane which in turn can encompass only three Syt1 C2B molecules (shown in purple, light grey and blue; marked by a dashed arc line). This ring-like organization naturally aligns the Syntaxin-binding hydrophobic pocket of the MUN domain with every third primary SNAREpin-binding interface of Syt1 C2B (light blue). (C) SVs contain ring-like hexamers of Syp (purple) which we suggest comprises the inner-most of the three concentric rings and template SNAREpin assembly based on the manner in which they position bound copies of the v-SNARE VAMP (not shown). (D) In this way, six SNAREpins (each a four-helix bundle of Syntaxin (red), SNAP25 (green) and VAMP (blue)) are envisioned to be assembled on the inner (Syt1 C2B) and potentially also outer (MUN) ring. The C-terminal ends of Syntaxin and VAMP (marked as 'C') are positioned inside the ring. One SNAREpin is marked with a black-yellow dashed line. Note that in this review we extend this concept to essentially replace each of the 6 SNAREpins with a ring of *pairs of SNAREpins* each trans-clamped by a bridging molecule of Complexin (Fig. 2). The additional 6 SNAREpins, a specialization for synaptic transmission, are proposed to account for the remarkable speed of this process.

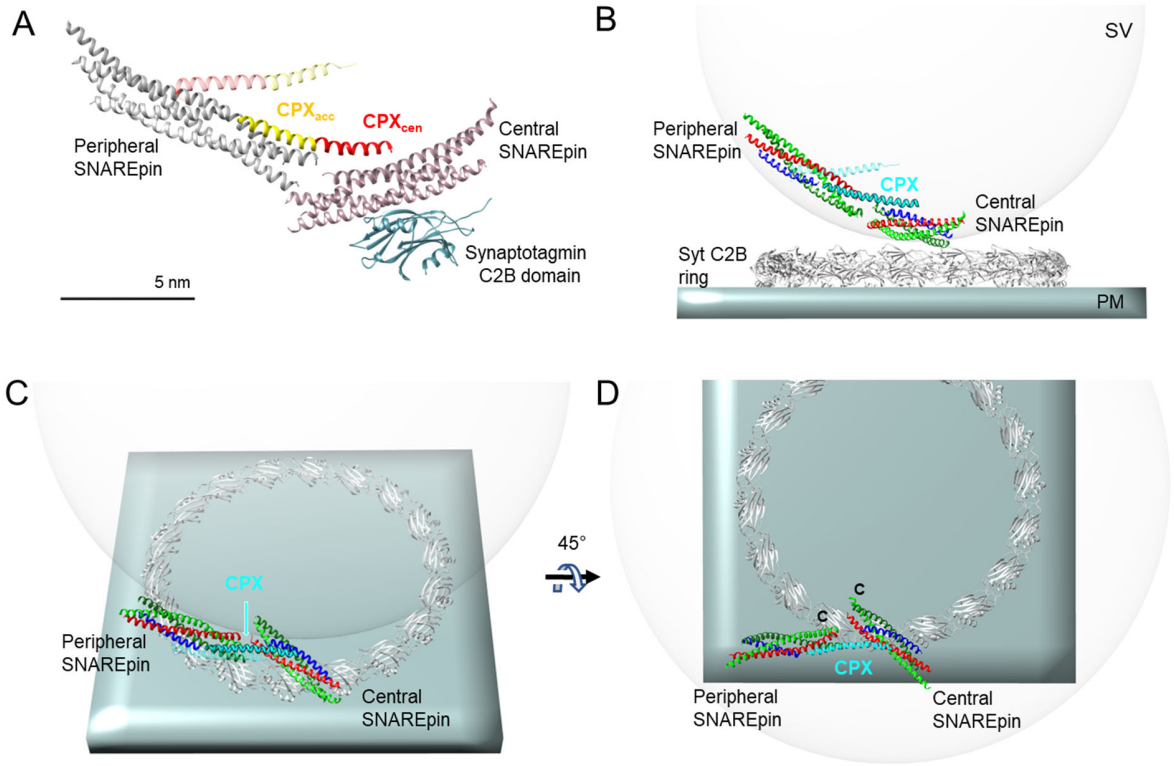

Figure 2. Trans-clamping of Central and Peripheral SNAREpins. (A) A model for the pre-fusion Complexin (Cpx)-Syt1-SNAREpin complex where one Cpx binds the central SNAREpin (light brown, marked as 'cSNAREpin') via its central helix (red) and extends to peripheral SNAREpin (light grey, marked as 'pSNAREpin') at an ~45° angle. The cSNAREpin is directly bound to and clamped by a Syt1 C_2B domain (light blue) through 'primary' because it is part of the Syt ring. The cSNAREpin is linked to the pSNAREpin by a bridging molecule of Cpx, whose central helix (CPX_{cen} red) is bound to the outer surface of the zippered (membrane-distal) portion of the cSNAREpin, and whose accessory helix (CPX_{acc} yellow) is bound to the unzippered (membrane-proximal) portion of the paired pSNAREpin. Another Cpx molecule (unmarked) binds exclusively to the peripheral SNAREpin via its central helix (red). This model was generated by superimposing two crystal structures, 5W5C [8] and 3RL0 [23]. (B-D) Side (B), tilted (C) and top (D) views of a single trans-clamped pair of SNAREpins and its bound Syt1 C_2B domain when the latter is incorporated into a ring according to the packing of Syt in helical tubular arrays [11; see Supporting Information Appendix Fig. S1A] and the cSNAREpin is positioned on C2B according to the X-ray structure [7]. These views reveal the peripheral positioning of pSNAREpins outside of the Syt ring oriented away from the PM approximately tangential to the surface of the SV. Individual SNAREs are color-coded (Syntaxin, SNAP25 and VAMP2 as red, green and blue respectively), and both Cpx molecules in cyan. 'C' marks the end of the SNAREpin containing the C-termini of VAMP2 and Syntaxin1. For simplicity, only one pair of trans-clamped SNAREpins is shown. However, a total of 6 such units, arranged symmetrically, are likely to be involved.

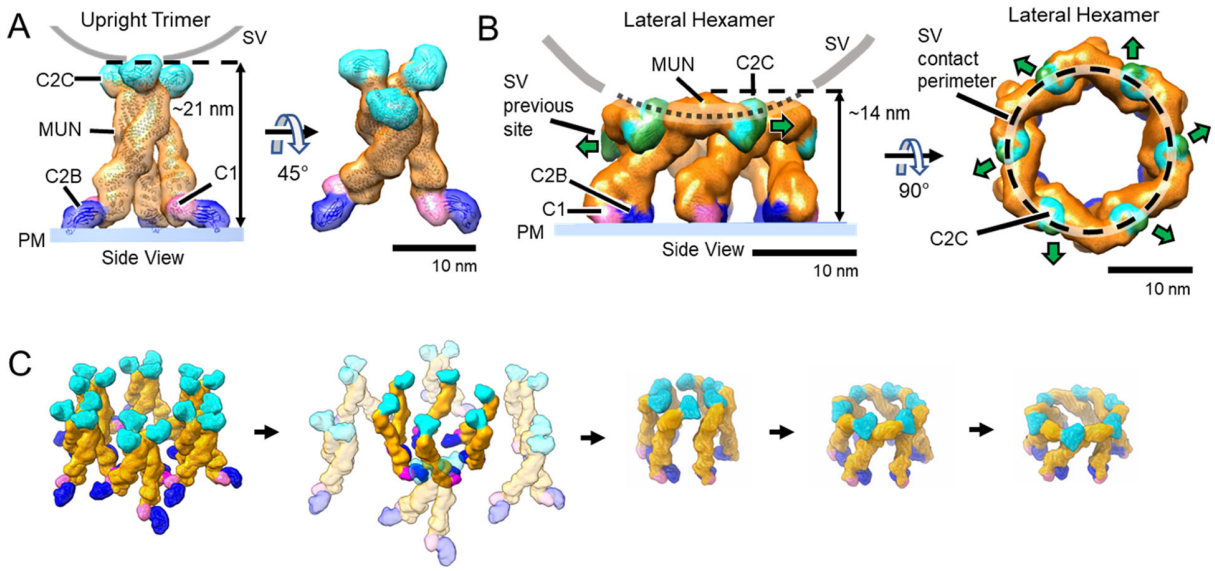

Figure 3. Structural transitions of upright Munc13 trimers into a lateral hexamer that are proposed to dock and prime SVs as they govern SNAREpin assembly. (A) Side view of an upright Munc13C (the C-terminal domains of Munc13 consisting of C_1-C_2B-MUN-C_2C) trimer (left) and a 45° tilted side view (right). Protein structures are shown in ribbon and corresponding synthetic 3D maps [36]. C_2B domains (dark blue) are shown attached to the PM (light blue slab), C_1 and MUN domains are shown in pink and orange respectively. C_2C domains (cyan) are oriented upward in the trimer, allowing the SV (grey, shown as 45 nm diameter) to bind. The separation of the SV from the PM is predicted to be ~21 nm in this geometry. Scale bar, 10 nm. (B) Side (left) and top (right) views of Munc13C assembled into a hexagonal cage within the crystal. In this configuration the surface of C_2C that had interacted with the SV (A) in the upright trimer (green) is now parallel to the PM (green arrow) and can no longer bind the SV. The SV is assumed to be directly atop the lateral hexamer cage of Munc13C. In this geometry the distance between the top of the hexagon cage and PM is ~14 nm and between the SV and the PM is predicted to be ~12 nm. In the top view (right panel) the line of contact between the SV and the hexamer cage is shown as a black dashed line. (C) A hypothetical model depicting several intermediate steps where the 6 innermost Munc13C molecules (see Fig. 5A for definitions) within an 18-mer hexamer of upright trimers could transition into a single lateral hexagonal cage. The 6 innermost Munc13 molecules are solid while, the outer Munc13s are in transparent colors. See Movie S2 https://www.pnas.org/doi/abs/10.1073/pnas.2121259119#supplementary-materials.

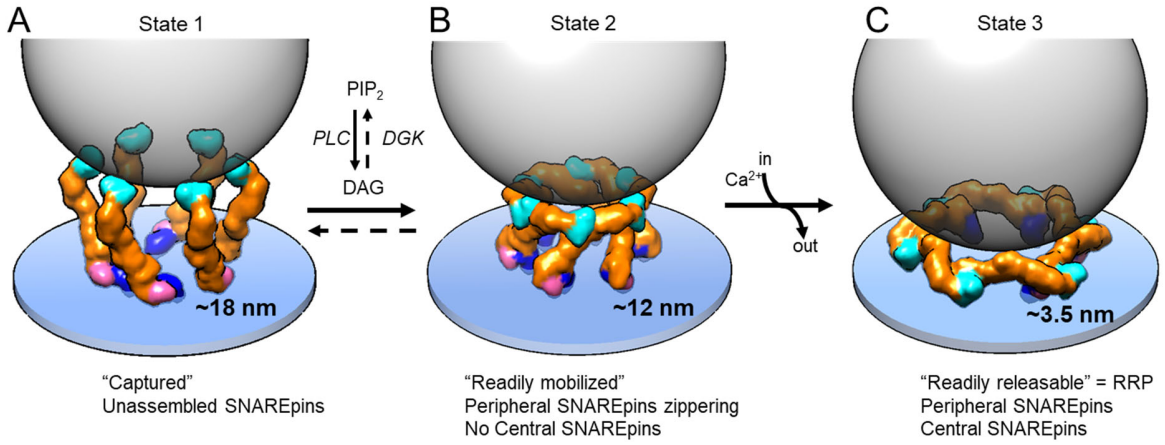

Figure 4. A model illustrating how the proposed structural transitions of Munc13 oligomer would enable synaptic vesicle capture, priming and clamping regulated by PIP_2, DAG and Ca^{++}. (A) State 1, the six innermost upright Munc13 molecules (each bound to the PM via PIP_2) capture an SV (shown as 45 nm diameter) via their C_2C domains (cyan). In this geometry, the distance between the bottom of the vesicle surface and PM is ~18 nm, a separation at which SNAREpins assembly intermediates can stably exist (see Fig. 7D and discussion in text). (B) DAG binding to the C_1 domain is proposed (Fig. 6) to trigger the transition (Fig. 3) of these innermost Munc13s from upright (open) to lateral (closed) conformations, thereby re-assembling into a lateral hexagonal cage (State 2). This also requires a concomitant rearrangement in all Munc13 protomers (discussed in text but not shown here). A catalytic pocket in the MUN domain which is required to open Syntaxin-Munc18 is occluded by direct contact with the neighboring C_2C domains, implying that SNARE assembly is auto-inhibited in the lateral hexamer [36] The SV and PM are now ~12 nm apart, which is close enough for peripheral SNAREpins to stably exist between the two membranes (discussed in text). (C) In State 3, meant to correspond to the ready-releasable pool as defined physiologically, the SV is measured by cryo-EM tomography to be ~3.5 nm away from the PM [10] within which SNAREpins are primed and clamped at the approximately half-zippered stage by Syt1 rings (not shown here for simplicity). The transition from state 2 to 3 is most likely facilitated by the Ca^{2+} influx which causes the Ca^{2+} binding loop of Munc13 C_2B to be inserted into the bilayer resulting in rotation to Munc13 towards the PM [36]. The positioning of Munc13 in State 3 is unknown but is shown here in a manner consistent with aforementioned rotation and the concept of an outer ring of MUN domains (Fig. 1).

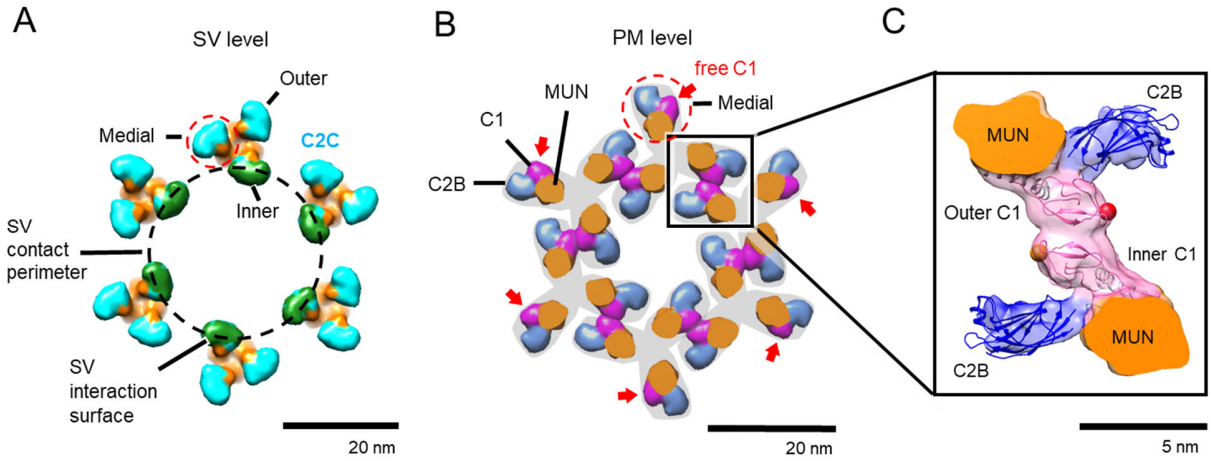

Figure 5. Non-equivalence of the three protomers of upright trimers of Munc13 resulting from asymmetrical binding of the synaptic vesicle. (A) Top view of the 18-mer hexagon (hexamer of upright trimers) showing only the 18 C_2C domains at the level of a docked 45 nm diameter SV (vesicle (black dashed circle). Only the Inner C2C (green) is positioned to enable contact with the vesicle surface. The Medial (cyan and circled in red dashed line) and Outer (cyan) C_2Cs are in non-equivalent geometries with respect to the SV surface. Scale bar, 20 nm. (B) View of a slice of the same structure just above and parallel to the PM where the C_2B (light blue) domains bind PIP_2 on the cytoplasmic surface of the PM. The PM attachment of one of the six Medial subunits in A at the level of the SV now at the level of the PM is encircled with a red dashed line. The C_1 domains of these Medial (magenta) subunits point radially outward where they are free of contacts. Scale bar 20 nm. (C) By contrast, the C1 domains of the Inner and Outer subunits are in direct contact just above the PM surface (Fig. 6A shows a side view). These anti-parallel contacts are responsible for organizing the upright trimers into the 18-mer hexagon. Scale bar 5 nm. Gray outlines denote the base of each trimer. Mun domains are in orange. Red and orange spheres denote the DAG binding pockets.

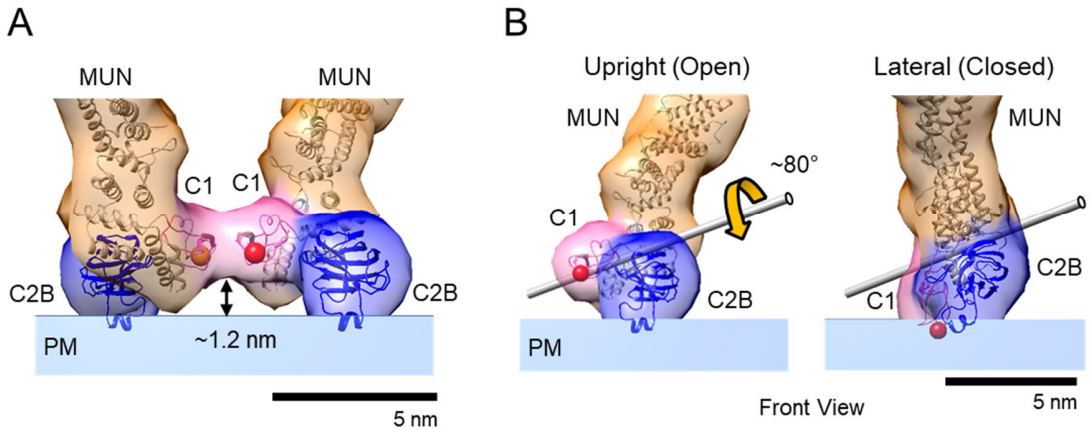

Figure 6. Open to Closed conformational switch of Munc13 stabilized by diacylglycerol (DAG) binding to C_1 domain when C2B is attached to the plasma membrane via PIP_2. (A) Side view of the C_1-C_1 link between neighboring upright trimers that assembles them into an 18-mer hexagon. Each such link consists of a symmetrical dyadic pair of contacting C_1 domains (pink). Importantly, they are ~1.2 nm (based on the phorbol ester bound PKC C1 structure, PDB: 1PTR) above the lipid bilayer surface (blue slab) and parallel to it. This positions their DAG binding pockets (red [facing above the page] and pink [facing below the page] spheres) to prevent simultaneous binding of DAG to the bilayer and to C_1, lowering overall affinity. (B) Front view showing the C_1, C_2B and a PM-proximal portion of MUN domains in their Open (left) and Closed (right) conformations which are present in Upright Trimers and Later Hexagons, respectively, in the crystal structure [36]. Open and Closed are related by a simple rigid body rotation in which C_2B (blue) remains fixed on the membrane and a rigid C_1-MUN (pink-orange) unit is rotated ~80^o toward the membrane around the axis indicated by the grey rod. This motion brings the DAG-binding surface of C_1 into direct contact with the lipid bilayer, permitting high affinity simultaneous binding of DAG by C_1 and the bilayer. It also adds contacts between C_1 and MUN with C_2B, further stabilizing the Closed conformation when attached to the membrane. Scale bar, 5 nm.

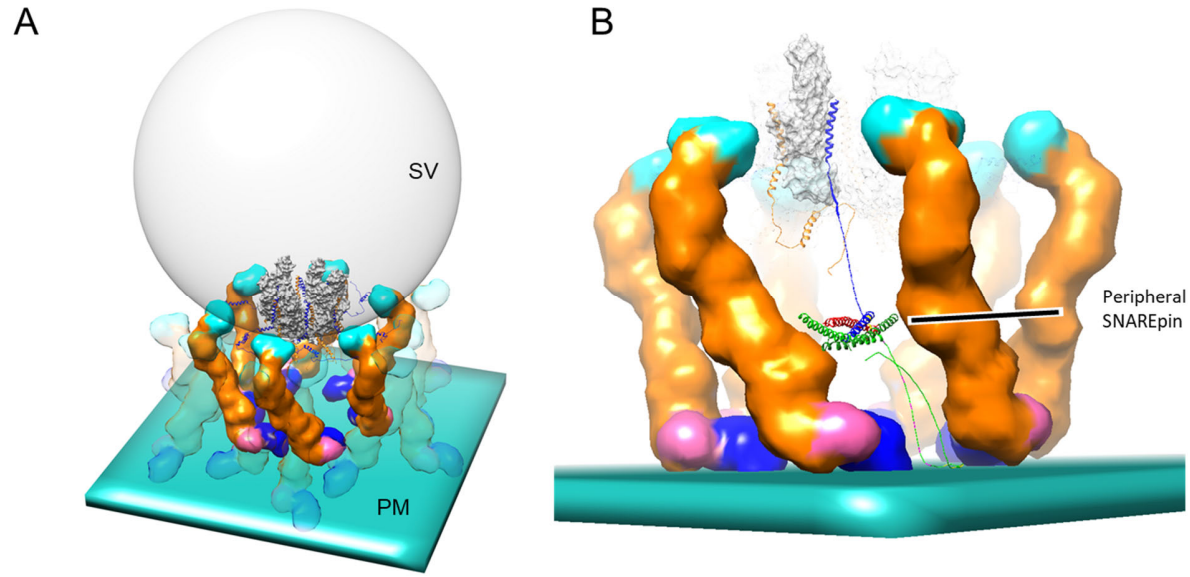

Figure 7. Asymmetrical positioning of the two copies of VAMP on Synaptophysin may result in structurally distinct Peripheral and Central SNAREpins. (A) 45 nm diameter synaptic vesicle (SV, grey sphere) is shown bound to the 6 Inner Munc13s within an 18-mer hexagon of Upright Trimers (the remainder of which are transparent). In this state (Fig. 4, State 1) the C_2B (blue) and C_1 (pink) domains are, respectively, on and above the plasma membrane (PM, blue slab) as detailed in Fig. 6A. A Synaptophysin (Syp, grey) hexamer within the SV bilayer is positioned symmetrically within the structure. (B) Side view showing a single subunit of the Syp hexamer with 2 copies of VAMP molecules emanating from it in the $VAMP_{12}$-Syp_6 complex. The exact location and contacts involved in this complex are unknown so the positioning of the VAMPs (the NMR-based structure of VAMP2 (PDB: 2KOG) [45] and $VAMP_{12}$-Syp_6 complex [32] were used as initial models) is arbitrary. The space between the 6 upright MUN domains retaining the SV is sufficient to accommodate one but not two SNAREpins which could explain why only 6 (peripheral) SNAREpins can assemble at this stage (State 1) or later in State 2 (Fig. S1). Alternatively, one copy of VAMP (orange) could be restricted from SNARE assembly by binding to another protein potentially Syp [30] leaving only the other copy (blue) free to assemble into a pSNAREpin. Modeling suggests that SNAREpins can zipper up to layer -1 [defined in ref. 43] in this geometry, even when their palmitoylated SNAP25 linker domains are inserted into the PM and that there is space for only one such SNARE complex to assemble.

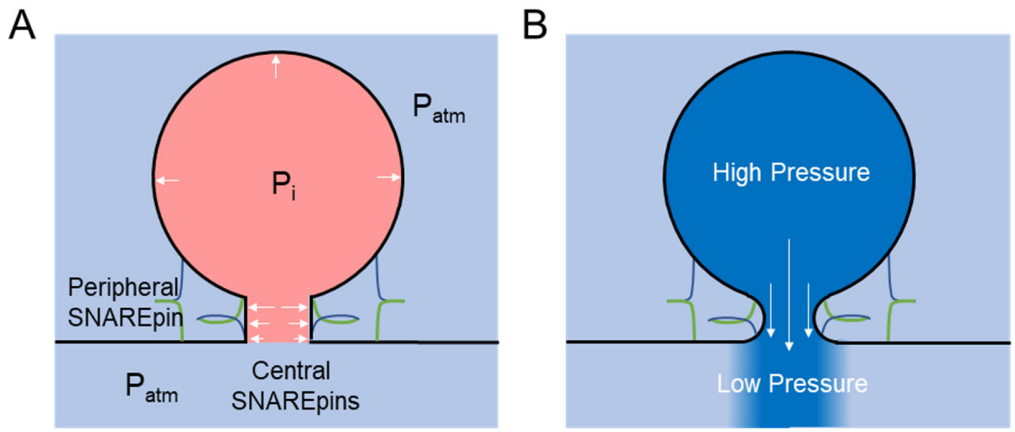

Figure 8. Peripheral SNAREpins may turbocharge neurotransmitter release following released by Ca^{++}. In the primed vesicle, pSNAREpins will raise the pressure inside the vesicle (Pi) higher than outside the vesicle (atmospheric pressure, P_{atm}), see Supplementary text. The fusion pore opens when sufficient central SNAREpins have terminally zippered, at which stage they cease to exert force. However, the peripheral SNAREpins which are not yet fully zippered continue to exert force pulling the vesicle toward the membrane. This transiently maintains the higher pressure inside the vesicle, see Supplementary Text and Figures S2-S4 for explanations, approximations, and limitations. (A) The pressure difference across the opening fusion pore (shown diagrammatically as a simple cylinder) results in a radially-directed outward force vector (white arrows) that is predicted to accelerate pore expansion to make fusion pore opening irreversible. (B). The same pressure difference across the open pore (while arrows) is predicted to create fluid flow that will express dissolved neurotransmitter out of the vesicle faster than simple diffusion.

References

1. Brunger, A.T., et al., *The pre-synaptic fusion machinery.* Curr Opin Struct Biol, 2019. **54**: p. 179-188.
2. Rothman, J.E., et al., *Hypothesis - buttressed rings assemble, clamp, and release SNAREpins for synaptic transmission.* FEBS Lett, 2017. **591**(21): p. 3459-3480.
3. Wang, J., et al., *Calcium sensitive ring-like oligomers formed by synaptotagmin.* Proc Natl Acad Sci U S A, 2014. **111**(38): p. 13966-71.
4. Wang, J., et al., *Circular oligomerization is an intrinsic property of synaptotagmin.* Elife, 2017. **6**: p. e27441.
5. Yang, X., et al., *Syntaxin opening by the MUN domain underlies the function of Munc13 in synaptic-vesicle priming.* Nat Struct Mol Biol, 2015. **22**(7): p. 547-54.
6. Xu, J., et al., *Mechanistic insights into neurotransmitter release and presynaptic plasticity from the crystal structure of Munc13-1 C1C2BMUN.* Elife, 2017. **6**: p. e22567.
7. Zhou, Q., et al., *Architecture of the synaptotagmin-SNARE machinery for neuronal exocytosis.* Nature, 2015. **525**(7567): p. 62-7.
8. Zhou, Q., et al., *The primed SNARE-complexin-synaptotagmin complex for neuronal exocytosis.* Nature, 2017. **548**(7668): p. 420-425.
9. Li, X., et al., *Symmetrical organization of proteins under docked synaptic vesicles.* FEBS Lett, 2019. **593**(2): p. 144-153.

10. Radhakrishnan, A., et al., *Symmetrical arrangement of proteins under release-ready vesicles in presynaptic terminals.* Proc Natl Acad Sci U S A, 2021. **118**(5): p. e2024029118.
11. Bello, O.D., et al., *Synaptotagmin oligomerization is essential for calcium control of regulated exocytosis.* Proc Natl Acad Sci U S A, 2018. **115**(32): p. E7624-E7631.
12. Ramakrishnan, S., et al., *High-Throughput Monitoring of Single Vesicle Fusion Using Freestanding Membranes and Automated Analysis.* Langmuir, 2018. **34**(20): p. 5849-5859.
13. Ramakrishnan, S., et al., *Synaptotagmin oligomers are necessary and can be sufficient to form a Ca(2+) -sensitive fusion clamp.* FEBS Lett, 2019. **593**(2): p. 154-162.
14. Bera, M., et al., *Molecular determinants of complexin clamping and activation function.* Elife, 2022. **11**: p. e71938.
15. Ramakrishnan, S., et al., *Synergistic roles of Synaptotagmin-1 and complexin in calcium-regulated neuronal exocytosis.* Elife, 2020. **9**: p. e54506.
16. Bera, M., et al., *Synaptophysin Chaperones the Assembly of 12 SNAREpins under each Ready-Release Vesicle.* bioRxiv, 2023: p. 2023.07.05.547834.
17. Takamori, S., et al., *Molecular anatomy of a trafficking organelle.* Cell, 2006. **127**(4): p. 831-46.
18. Tagliatti, E., et al., *Synaptotagmin oligomers clamp and regulate different modes of neurotransmitter release.* Proc Natl Acad Sci U S A, 2020. **117**(7): p. 3819-3827.
19. Courtney, K.C., et al., *Synaptotagmin 1 oligomerization via the juxtamembrane linker regulates spontaneous and evoked neurotransmitter release.* Proc Natl Acad Sci U S A, 2021. **118**(48): p. e2113859118.
20. Manca, F., et al., *SNARE machinery is optimized for ultrafast fusion.* Proc Natl Acad Sci U S A, 2019. **116**(7): p. 2435-2442.
21. Heo, P., et al., *Nascent fusion pore opening monitored at single-SNAREpin resolution.* Proc Natl Acad Sci U S A, 2021. **118**(5): p. e2024922118.
22. Jaczynska, K., et al., *Analysis of tripartite Synaptotagmin-1-SNARE-complexin-1 complexes in solution.* FEBS Open Bio, 2023. **13**(1): p. 26-50.
23. Kummel, D., et al., *Complexin cross-links prefusion SNAREs into a zigzag array.* Nat Struct Mol Biol, 2011. **18**(8): p. 927-33.
24. Choi, U.B., et al., *Complexin induces a conformational change at the membrane-proximal C-terminal end of the SNARE complex.* Elife, 2016. **5**: p. e16886.
25. Maximov, A., et al., *Complexin controls the force transfer from SNARE complexes to membranes in fusion.* Science, 2009. **323**(5913): p. 516-21.
26. Radoff, D.T., et al., *The accessory helix of complexin functions by stabilizing central helix secondary structure.* Elife, 2014. **3**: p. e04553.
27. Cho, R.W., et al., *Genetic analysis of the Complexin trans-clamping model for cross-linking SNARE complexes in vivo.* Proc Natl Acad Sci U S A, 2014. **111**(28): p. 10317-22.
28. Malsam, J., et al., *Complexin Suppresses Spontaneous Exocytosis by Capturing the Membrane-Proximal Regions of VAMP2 and SNAP25.* Cell Rep, 2020. **32**(3): p. 107926.
29. Kalyana Sundaram, R.V., et al., *Native Planar Asymmetric Suspended Membrane for Single-Molecule Investigations: Plasma Membrane on a Chip.* Small, 2022. **18**(51): p. e2205567.
30. Edelmann, L., et al., *Synaptobrevin binding to synaptophysin: a potential mechanism for controlling the exocytotic fusion machine.* EMBO J, 1995. **14**(2): p. 224-31.
31. Washbourne, P., G. Schiavo, and C. Montecucco, *Vesicle-associated membrane protein-2 (synaptobrevin-2) forms a complex with synaptophysin.* Biochem J, 1995. **305**(Pt 3): p. 721-4.
32. Adams, D.J., C.P. Arthur, and M.H. Stowell, *Architecture of the Synaptophysin/Synaptobrevin Complex: Structural Evidence for an Entropic Clustering Function at the Synapse.* Sci Rep, 2015. **5**: p. 13659.

33. White, D.N. and M.H.B. Stowell, *Room for Two: The Synaptophysin/Synaptobrevin Complex.* Front Synaptic Neurosci, 2021. **13**: p. 740318.
34. Janz, R., et al., *Essential roles in synaptic plasticity for synaptogyrin I and synaptophysin I.* Neuron, 1999. **24**(3): p. 687-700.
35. Raja, M.K., et al., *Elevated synaptic vesicle release probability in synaptophysin/gyrin family quadruple knockouts.* Elife, 2019. **8**: p. e40744.
36. McMahon, H.T., et al., *Synaptophysin, a major synaptic vesicle protein, is not essential for neurotransmitter release.* Proc Natl Acad Sci U S A, 1996. **93**(10): p. 4760-4.
37. Grushin, K., et al., *Munc13 structural transitions and oligomers that may choreograph successive stages in vesicle priming for neurotransmitter release.* Proc Natl Acad Sci U S A, 2022. **119**(7): p. e2121259119.
38. Papantoniou, C., et al., *Munc13- and SNAP25-dependent molecular bridges play a key role in synaptic vesicle priming.* Sci Adv, 2023. **9**(25): p. eadf6222.
39. Wang, S., et al., *Conformational change of syntaxin linker region induced by Munc13s initiates SNARE complex formation in synaptic exocytosis.* EMBO J, 2017. **36**(6): p. 816-829.
40. Ma, C., et al., *Munc13 mediates the transition from the closed syntaxin-Munc18 complex to the SNARE complex.* Nat Struct Mol Biol, 2011. **18**(5): p. 542-9.
41. Bera, M., et al., *Two successive oligomeric Munc13 assemblies scaffold vesicle docking and SNARE assembly to support neurotransmitter release.* bioRxiv, 2023: p. 2023.07.14.549017.
42. Sundaram, R.V.K., et al., *Novel Roles for Diacylglycerol in Synaptic Vesicle Priming and Release Revealed by Complete Reconstitution of Core Protein Machinery.* bioRxiv, 2023: p. 2023.06.05.543781.
43. Jiao, J., et al., *Munc18-1 catalyzes neuronal SNARE assembly by templating SNARE association.* Elife, 2018. **7**: p. e41771.
44. Stepien, K.P., et al., *SNARE assembly enlightened by cryo-EM structures of a synaptobrevin-Munc18-1-syntaxin-1 complex.* Sci Adv, 2022. **8**(25): p. eabo5272.
45. Ellena, J.F., et al., *Dynamic structure of lipid-bound synaptobrevin suggests a nucleation-propagation mechanism for trans-SNARE complex formation.* Proc Natl Acad Sci U S A, 2009. **106**(48): p. 20306-11.
46. Li, F., et al., *A half-zippered SNARE complex represents a functional intermediate in membrane fusion.* J Am Chem Soc, 2014. **136**(9): p. 3456-64.
47. Sutton, R.B., et al., *Crystal structure of a SNARE complex involved in synaptic exocytosis at 2.4 A resolution.* Nature, 1998. **395**(6700): p. 347-53.
48. Kalyana Sundaram, R.V., et al., *Munc13 binds and recruits SNAP25 to chaperone SNARE complex assembly.* FEBS Lett, 2021. **595**(3): p. 297-309.
49. Harper, C.B., E.M. Blumrich, and M.A. Cousin, *Synaptophysin controls synaptobrevin-II retrieval via a cryptic C-terminal interaction site.* J Biol Chem, 2021. **296**: p. 100266.
50. Miki, T., et al., *Two-component latency distributions indicate two-step vesicular release at simple glutamatergic synapses.* Nat Commun, 2018. **9**(1): p. 3943.
51. Neher, E. and N. Brose, *Dynamically Primed Synaptic Vesicle States: Key to Understand Synaptic Short-Term Plasticity.* Neuron, 2018. **100**(6): p. 1283-1291.
52. Hui, E., J. Bai, and E.R. Chapman, *Ca2+-triggered simultaneous membrane penetration of the tandem C2-domains of synaptotagmin I.* Biophys J, 2006. **91**(5): p. 1767-77.
53. Lin, K.H., H. Taschenberger, and E. Neher, *A sequential two-step priming scheme reproduces diversity in synaptic strength and short-term plasticity.* Proc Natl Acad Sci U S A, 2022. **119**(34): p. e2207987119.
54. Zhang, Y., *Energetics, kinetics, and pathway of SNARE folding and assembly revealed by optical tweezers.* Protein Sci, 2017. **26**(7): p. 1252-1265.